

JUL 3 4 1978

Item 830-H-15

NASI.60:1239

NASA Technical Paper 1239

**ORIGINAL
COMPLETED**

**An Evaluation of In Situ Ozone
Sensor Performance During
a Cold Frontal Passage**

C. L. Parsons

JULY 1978

NASA

34

NASA Technical Paper 1239

**An Evaluation of In Situ Ozone
Sensor Performance During
a Cold Frontal Passage**

C. L. Parsons
Wallops Flight Center
Wallops Island, Virginia



National Aeronautics
and Space Administration

**Scientific and Technical
Information Office**

1978

EVALUATION OF IN SITU OZONE SENSOR
PERFORMANCE DURING A COLD FRONTAL PASSAGE

C. L. Parsons
NASA/Wallops Flight Center
Wallops Island, VA 23337

SUMMARY

The capabilities of the Electrochemical Concentration Cell ozonesonde for measuring the vertical profile of atmospheric ozone were studied during a three-day experiment at Wallops Island, Virginia, and Norfolk, Virginia. Using ancillary measurements by Dasibi Corporation Optical Ozone Monitors at the surface and the Wallops Island Dobson spectrophotometer, it was concluded that the ozonesonde measures the total ozone overburden to within 10% of the real value.

By releasing the balloon-borne instruments at a rate of four per day at each of the two sites, an indication was obtained of the temporal and spatial scales of atmospheric ozone variability. No significant effects of a weak cold front passage or of the loss of insolation at night were seen. An isolated incident of anomalously high ozone concentration at the peak of the profile has been attributed to sporadic instrument performance effects. The data base currently available is not adequate for determining an exact cause of the anomaly.

INTRODUCTION

With the publication of an article by Molina and Rowland¹ in Nature in 1974, a new impetus has been added to the search for knowledge of the full influence of ozone on atmospheric processes. The essence of their hypothesis was that chlorofluoromethanes (CFM's), organic compounds generated by man for use in aerosol spray cans, refrigeration, and air conditioning, are capable of destroying ozone in the stratosphere. This family of useful compounds, although chemically inert at the surface, was conjectured to be dissociated in the upper atmosphere by the same ultraviolet radiation that is filtered by the ozone layer. The chlorine atom released is believed to be highly proficient at the destruction of ozone. With a reduction in the amount of ozone aloft, more ultraviolet radiation may

be allowed to reach the earth's surface with a potential net increase in the occurrence of skin cancer and other maladies in humans as well as disturbances in the earth's ecology.²

Ozone is also subject to destruction by chemical compounds in the nitrogen oxide family. With the exponential rise in the use of nitrogen fertilizers in the "Green Revolution,"³ these may be of even more significant impact than are CFCs. Crutzen^{3,4} and Johnston⁵ also identified another source of NO in the upper atmosphere as high flying supersonic aircraft (SST's).

Concerns over the inadvertent modification of the climate of the stratosphere by chlorofluoromethanes led to the formation of the Interagency Task Force on Inadvertent Modification of the Stratosphere (IMOS) in 1975, co-sponsored by the Federal Council for Science and Technology and the Council on Environmental Quality.⁶ The potential effects of a fleet of supersonic aircraft led to the 1970-1974 Climatic Impact Assessment Program (CIAP) in the Department of Transportation.⁷

These and other studies in recent years have consistently concluded that measurements of stratospheric chemical constituents are too infrequent and too sparse to satisfy the requirements of an ambitious monitoring program of the sort outlined in the national climate program recently recommended⁸ by the Interdepartmental Committee for Atmospheric Sciences (ICAS) of the Federal Coordinating Council for Science, Engineering and Technology. In 1974, the Joint Organizing Committee of the Global Atmospheric Research Program (GARP) convened a conference in Stockholm, Sweden, to formulate requirements for "understanding the physical basis of climate," the second objective of GARP. Their recommendations⁹ included requirements for an intensive study of atmospheric chemical interactions and the long-term monitoring of the ozone content of the stratosphere. Researchers are faced with the uncomfortable yet highly challenging task of making highly accurate measurements of an unknown number of important atmospheric constituents whose concentrations are variable in time and space. The variability is partly natural but may be influenced by man. Assuredly, the former effects are much larger than the latter for the case of ozone. For example, for a typical mid-latitude station, day-to-day variations in total ozone overburden average about 10% in winter and 5% in summer. Superimposed on this is an approximately 25% annual variation, a 2% quasi-biennial oscillation, and possible long-term trends amounting to as much as 5% per decade.¹⁰

How can man's influence be detected if all of these natural variations are poorly understood? Even if the natural driving forces are understood, do we have the measurement capability of detecting a man-made 1-2% ozone reduction over a period of some 10 years? To determine how well we understand the natural variation of ozone and our measurement capabilities would require a research activity of the scope of GARP. As a first step in that direction, the goal of this experiment was to evaluate the performance of in-situ ozone sensors in the real atmosphere. In-situ instrumentation is currently better under-

stood than are the satellite-borne sounders under development for NIMBUS-G and TIROS-N, for example, and though lacking in global coverage, they will be essential for verifying the performance of satellite instrumentation and for relating the data from one satellite to that of another. At the present, their accuracies are the best available and the vertical resolution of balloon and rocket-borne sensors will never be matched by remote sounders.

To examine the natural variability of ozone on all time scales, horizontal scales, and at all altitudes from the surface through the stratosphere is an enormous task. Only a limited investigation of temporal, spatial, and vertical variability is economically and logistically feasible in advance of GARP or a national climate program but studies using equipment and facilities to their ultimate potential should be performed to establish the baseline capability of ozone measurements. The following section describes the equipment used in the experiment and gives details about the experiment's structure.

EXPERIMENTAL TECHNIQUE

Instrumentation

As the only station routinely flying balloon-borne ozonesondes in the United States at the present time, NASA's Wallops Flight Center (WFC) has developed considerable expertise in the collection of high-quality in-situ ozone profile data. The instrumentation available for use in this experiment at Wallops Flight Center includes balloon-borne electrochemical ozonesondes, surface-based Dasibi Corporation Optical Ozone Monitors, and a Dobson spectrophotometer. This collection represents the state-of-the-art in in-situ ozone measurement capability. A brief description of each sensor system follows with major emphasis in the discussions placed on the quality of the measurements produced.

Dobson Spectrophotometer.¹¹ This instrument has served as the standard for the measurement of total atmospheric ozone for a number of decades. In a recent study, Thomas and Holland¹² have investigated the effects of two sources of possible error in the Dobson instrument measurements. These are the uncertainty in the temperature sensitivity of the ozone absorption coefficients and the variable effects of scattered radiation. Their conclusions were that for a well-maintained instrument, the atmospheric temperature variability may result in an error of $2.4 \pm 0.5\%$ for a coupled A-D line pair measurement, the configuration recommended by the World Meteorological Organization. Similarly, the combined influence of aerosol attenuation and scattered radiation was found to cause an error of less than 1% again for an A-D coupled measurement. In conclusion, Thomas and Holland state that an error of 5% should be expected in the use of Dobson spectrophotometer data.

The Wallops Dobson instrument is well-maintained and is regularly calibrated against the standard ozone spectrophotometer maintained by NOAA at Boulder, Colorado. In these tests, the agreement is generally within 1% (private communication from W. Komhyr, NOAA, Boulder, Colorado). Hence, the total ozone measurements produced in this experiment are of high precision and reasonably high accuracy.

Dasibi Corporation Optical Ozone Monitor.¹³ This commercially available instrument served as the surface ozone sensor in this experiment. A self-contained unit, it measures the concentration of ozone in the ambient atmosphere by sensing the absorption of ultraviolet (UV) radiation by an ozonized air sample. Recently, studies have been conducted to compare various commonly-used techniques for measuring surface ozone. The results of one investigation¹⁴ were that either the UV absorption method or gas phase titration were capable of absolute measurements. On the other hand, the 1 percent neutral buffered potassium iodide (NBKI) technique used by the Environmental Protection Agency (EPA), the 2 percent NBKI method of the California Air Resources Board, and a 1 percent unbuffered potassium iodide technique used by the Los Angeles Air Pollution Control District all yield ozone measurements 1 to 13 percent higher than the absolute levels for dry air. For higher humidities, these latter methods are too high by some 15 to 30 percent.

The Dasibi instrument, of course, is not a laboratory-grade device. It is, however, commonly used as a secondary standard with frequent comparisons against a primary to maintain its calibration. This was the technique used in this experiment. The primary used was the 3 m cell maintained by Drexel University.¹⁵ When referenced back to an absolute ultraviolet absorption measurement, the Wallops field Dasibi instrument calibration is

$$[O_3]_{WAL} = -1 + 1.03 [O_3]_{UV} \quad (1)$$

where the ozone concentrations are expressed in parts per billion by volume (ppb). The uncertainty in an absolute measurement from the Wallops Dasibi instrument is on the order of 1-2 ppb (private communications from Arnold Torres, Drexel University, Philadelphia, Pennsylvania). The precision quoted by the instrument manufacturer¹⁶ is $\pm 1\%$ or 1 digit on the 0 to 999 ppb display, whichever is greater, and the drift is stated to be less than $\pm 1\%$ over a three day period. Hence, with the absolute calibration the Wallops surface ozone measurements are of high quality.

Electrochemical Concentration Cell (ECC) Ozonesonde. The ECC ozonesonde was developed by W. Komhyr^{16,17} for use in measuring from a balloon platform the variation of ozone concentration with altitude. The sensor is based on an iodine/iodide redox cell in which ozone is consumed in the oxidation of iodide ions to molecular iodine. The latter is quickly converted back to the iodide form in a reaction driven by the iodide concentration differential that exists between the cell anode and cathode. The electrical current

produced is proportional to the mass flow rate of ozone into the cell and is detected and transmitted via telemetry back to a ground-based receiver.

The data quality of the sensor has recently been evaluated by Torres and Bandy.¹⁵ Using the Wallops Dobson spectrophotometer as a reference, comparisons with the integrated total ozone content measured by ECC ozonesondes released during 1977 have revealed that the balloon sensors underestimated the total ozone overburden by 5.7% with an uncertainty in the comparison of $\pm 8.5\%$.

Ancillary Data. The following data was gathered in support of the ozone data collection. The National Weather Service (NWS) support facility located at Wallops Flight Center routinely collects radiosonde temperature and dew point profiles at synoptic times and windspeed, direction, pressure, humidity, and temperature-surface data continuously. Additionally, standard radiosonde temperature, dew point, windspeed, and direction profiles were secured from the NWS for all eastern United States stations.

Strategy

With this information available, an experiment was designed with the following components. To verify the accuracy and repeatability numbers quoted above for the instruments, an inter-instrument comparison was included. For example, the surface readings from the ECC ozonesonde profiles are compared with Dasibi measurements taken nearby, and the integrated ECC ozonesonde profile overburden measurements are compared with the Dobson spectrophotometer data. No adjustment of the ozonesonde profiles to the Dobson readings was used and independent comparisons are thereby possible.

To examine the day-to-day variability of both total ozone and ozone concentration with height, multiple launches were made. With four balloons per day for the three days of the experiment, it is possible to examine both the day-to-day changes and the diurnal variation of ozone!

Finally, to examine the spatial variability of ozone, two stations were used for the ECC ozonesonde balloon releases. In addition to the existing launch facility at WFC, a portable unit was located at Norfolk International Airport for the experiment, and simultaneous balloon releases were made at each site.

In summary, the experiment consisted of data collected to facilitate inter-instrument, inter-site, and inter-launch comparisons. To ensure that reasonable meteorological conditions existed during the period of data collection, the scheduling of the balloon releases, the only non-routine activity of the experiment, was based on the imminent approach of a cold front. Following a discussion of these meteorological conditions in considerable detail in the next section, the results of the experiment's comparisons as a function of weather will be presented.

DATA COLLECTION

Synoptic Conditions

Figure 1 contains several items that help illustrate the movement of a late summer cold front across the eastern United States from September 9-11, 1977. The shaded and cross-hatched areas are taken from an SMS infrared image taken at 1030 GMT on September 9, and, therefore, are indications of cloud-top altitudes. The black areas are the lowest and hence warmest cloud-tops, the hatched regions represent higher cloud development, and the clear areas indicate maximum storm intensity. At the time of the photograph, the low pressure system was located over the Great Lakes and the trailing cold front stretched to the southwest across Lake Michigan, northern Missouri, and Kansas. The other meteorological feature of interest is the remains of tropical storm Babe which had moved across the southeastern United States after its landfall on September 4. The position of the cold front at synoptic times during the following two days is shown by the dashed lines in Figure 1. From surface data taken at WFC, the surface front passed off the east coast at 0315 GMT, September 11, 1977.

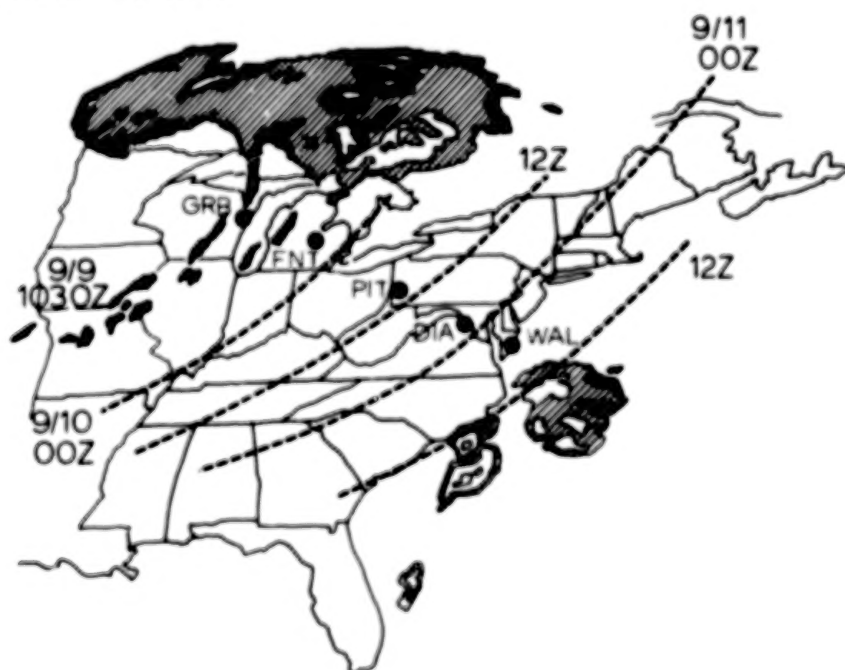


Figure 1. The progression of a cold front across the eastern United States during September 9-11, 1977. Data from the five radiosonde stations are used in subsequent isentropic cross section analyses.

The interrelation of meteorological conditions with total ozone content has been recognized for several decades. Dobson¹⁸ reported in the 1920's that outbreaks of cold

air coincided with increased total ozone amount measurements. In terms of the classical representation of cyclones and anticyclones, he also mapped the regions of highest total ozone overburden just behind the cold front and those with the smallest overburden ahead of the warm front in an extratropical cyclone. In anticyclones, a zone of depressed ozone amount was found to be typically located in the warm sector.

In order that the day-to-day variability of both the total ozone overburden and the ozone concentration as a function of height could be discerned during the changing synoptic conditions resulting from the September 11 cold frontal passage, a detailed picture of the front's structure throughout the period was necessary. The most useful representation has been found to be the vertical isentropic cross section,¹⁹ a side view of the atmosphere containing isolines of potential temperature. The most useful property of these isentropic surfaces is that they "crowd up" in stable zones, such as in frontal zones and near jet streams. By orienting the plane of the cross section along a line on the earth's surface normal to the cold front, a side view of the front's structure results. Various examples of this type of analysis are found in the literature. Staley²⁰ used isentropic analyses to demonstrate that extrusions of stratospheric air into the troposphere occur along and in corridors of isentropic surfaces where the boundary between the stratosphere and the troposphere deforms, becomes vertical in the core of the jet stream, and subsequently folds beneath the core of the jet.²¹ Danielsen^{22,23} has shown that ozone transport from stratosphere to troposphere also occurs in these corridors. As a final example of isentropic analysis usage, Frank and Barber²⁴ have recently studied in considerable detail the evolution of frontal systems on a time scale not usually obtainable during NASA's Atmospheric Variability Experiment (AVE II). Their data collection rate of 8 soundings per day enabled them to monitor changes in frontal intensity by the processes of frontogenesis and frontolysis.

For the particular orientation of the frontal system shown in Figure 1, a baseline normal to the surface front and falling on Wallops Island, Virginia (WAL), also lies nearby the standard radiosonde stations at Green Bay, Wisconsin (GRB), Flint, Michigan (FNT), Pittsburgh, Pennsylvania (PIT), and Dulles International Airport (DIA). These locations are indicated in Figure 1 by the black circles. Using radiosonde data collected at these sites during the experiment, isentropic cross sections were produced by linearly interpolating the significant level data, both vertically and horizontally, and contouring the values entered in the resulting equally-spaced grid. It was assumed for the analysis that the five reporting stations were spaced at equal intervals along the baseline. Figures 2-5 show the isentropic cross sections for 0000 GMT, September 10; 1200 GMT, September 10; 0000 GMT, September 11; and 1200 GMT, September 11. Superimposed on these charts are contour lines of constant windspeed. Only the component of the wind oriented normal to the baseline (or parallel to the surface front) is pictured. The heavy, dashed line indicates the altitude of the tropopause as indicated in the radiosonde data.

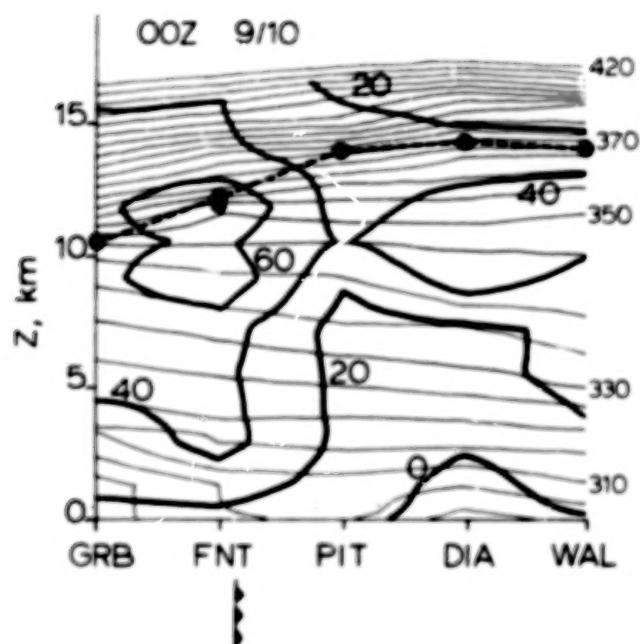


Figure 2. Isentropic cross section analysis for 0000 GMT, September 10, 1977. The light solid lines are isentropes in $^{\circ}\text{K}$ and the heavy solid lines are isopleths of windspeed in knots tangential to the cold front. The dashed line connects the reported locations of the tropopause.

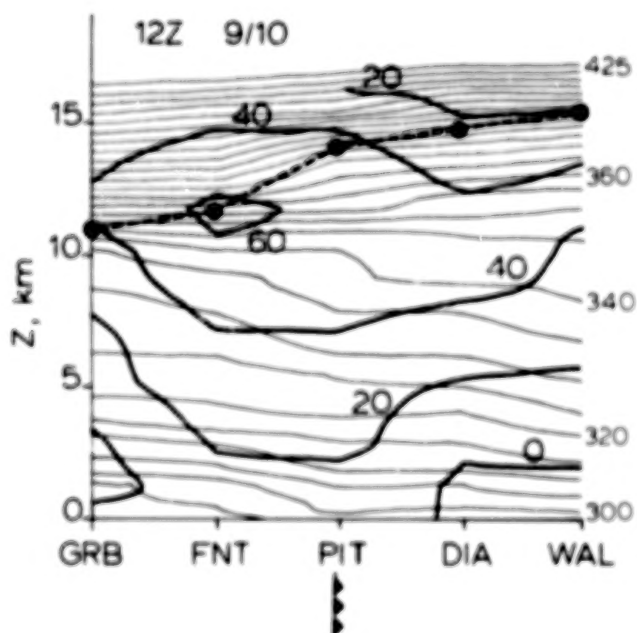


Figure 3. Isentropic cross section analysis for 1200 GMT, September 10, 1977.

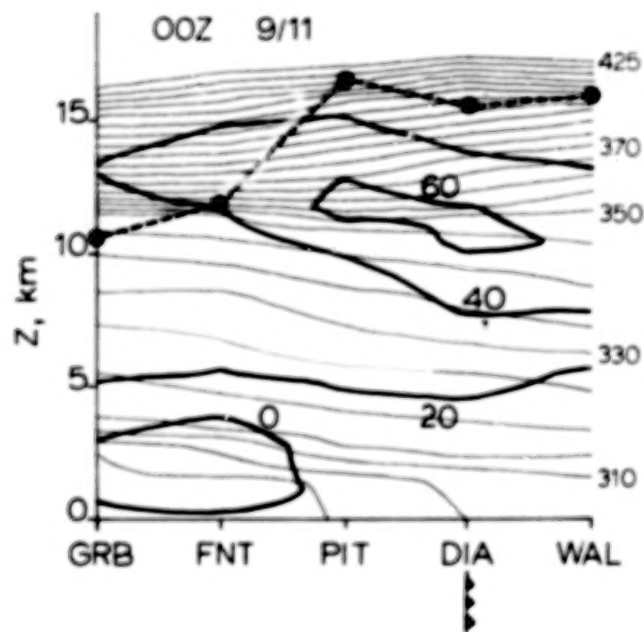


Figure 4. Isentropic cross section analysis for 0000 GMT, September 11, 1977.

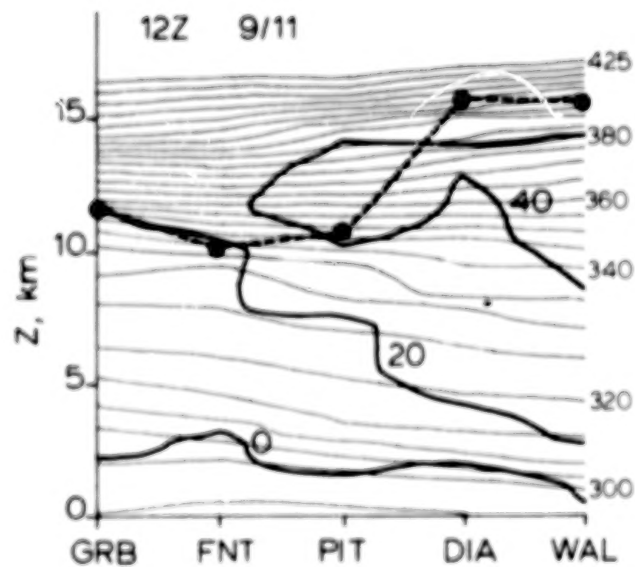


Figure 5. Isentropic cross section analysis for 1200 GMT, September 11, 1977.

In Figure 2, it can be seen that at Flint, Michigan, the location of the surface front at the start of data collection, a well-defined jet stream existed with a maximum normal-component windspeed of about 80 knots but no extrusion of stratospheric air beneath the jet can be seen. In the subsequent figures, the maximum windspeed at the core of the jet stream decreases as the frontal system in the upper troposphere weakens and moves to the southeast across the cross sections. At 1200 GMT, September 10, the surface front has passed Pittsburgh and the peak winds are only in excess of 60 knots. In Figure 4, the windspeed maximum is relatively unchanged but the location of the jet is near Dulles International Airport. By the time the surface front has moved over the Atlantic Ocean, the normal component of the windspeed bears no resemblance to an upper-air jet. In no instance was there observed an extrusion of stratospheric air and from surface stations along the baseline, there were no reports of precipitation.

Data Collection Summary

The ECC ozonesondes were, as mentioned previously, nominally released in pairs, one from Wallops Island, Virginia, and the other from Norfolk International Airport. In Table I, the pairs are listed together with comments concerning their suitability and balloon burst altitudes. Although some of the sondes did not reach the burst altitude hoped for (30 km), there are ten pairs of balloon ozonesonde data records for which inter-site comparisons have been made. The remainder of this report discusses the data collected routinely by the Wallops Dasibi and the Wallops Dobson spectrophotometer and the profile data from the ECC ozonesondes.

SURFACE DASIBI DATA

In Figure 6, the ozone concentration as measured by the WFC Dasibi instrument is contrasted with windspeed and dewpoint temperature data taken by the NWS support facility located also at WFC. The passage of the front at 0315 GMT is readily apparent in the rapid drop in humidity. Prior to the frontal passage, the windspeed was calm for a period of some 3-1/2 hours. Coincidentally, the ozone concentration underwent a sharp reduction marked by an unusually high level of "noisiness." Upon the passage of the front, a more normal record at its previous elevated level was resumed.

To examine the behavior of surface ozone over a longer period of time around the passage of the front, the WFC Dasibi data record was compared with similar recordings from Dasibi instruments located at Wachapreague, Virginia, a rural setting approximately 40 km

TABLE I. Inter-Site Balloon Ozonesonde Comparison Data

Date	Nominal Release Time (GMT)	Wallops Sonde		ORF Sonde	
		Number	Burst Pressure (mb)	Number	Burst Pressure (mb)
9/9	2000	3A-081**	6.4	3A-169	13.0
9/10	0200	3A-153	10.0	3A-170	7.6
9/10	0600	3A-158	4.6	3A-171	7.0
9/10	1500	3A-159	9.4	3A-181	13.8
9/10	2000	3A-167***	8.0	3A-183*	52.0
9/11	0200	3A-182	12.0	3A-185	6.2
9/11	0600	3A-192	4.0	3A-186	5.3
9/11	1500	3A-194	11.5	3A-187	5.0
9/11	2000	3A-195	7.5	3A-188	6.9
9/12	0200	3A-199	14.4	3A-189	2.9
9/12	0600	3A-201	7.4	3A-190	4.4
9/12	1500	3A-202	5.5	3A-191	4.6

* This balloon burst prematurely. It was replaced by sonde No. 3A-184 which was released at 2242 GMT, September 10. Unfortunately, it too burst at a low altitude of 26.2 mb.

** 3A-081 apparently suffered an instrument malfunction. The problem has not been identified but its measured ozone maximum concentration of 80 μ mb at about 24.5 km is inconsistent with the typical value of approximately 140 μ mb usually observed at WFC.

*** This sonde suffered a data dropout period between 82 and 37.6 mb of altitude. The remainder of the data record seems legitimate.

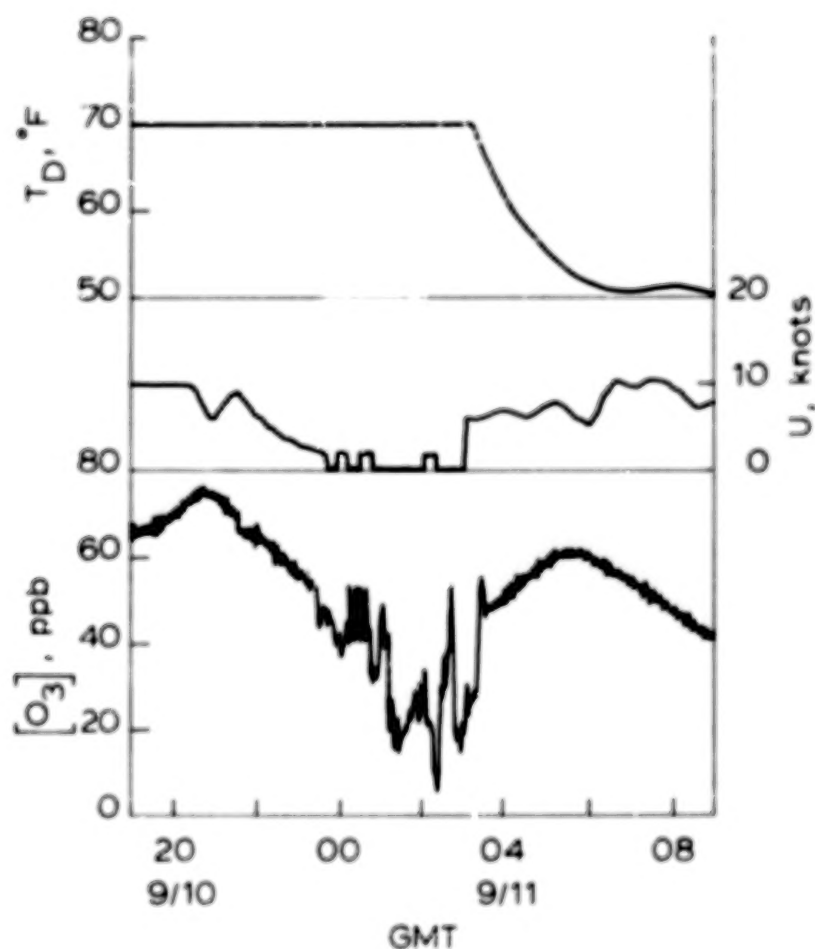


Figure 6. Time histories of dewpoint temperature, T_D , windspeed, U , and surface ozone concentration, $[O_3]$, during the cold frontal passage in the evening of September 10, 1977.

southwest of WFC, and at Norfolk International Airport, Norfolk, Virginia. The three records are superimposed in Figure 7. It can be seen that the effect of the cold front appears to be limited to the 4-5 hours immediately preceding its passage as all three stations experienced reductions in ozone concentration during the period of calm winds. During the following day, an early morning minimum occurred as usual around 0700 EST and a typical maximum near 1700 EST followed. No effects of the frontal passage during September 11, 1977, can be seen. The Wachapreague and Norfolk Airport data were provided by Mr. John Salop of the Virginia Air Pollution Control Board, Virginia Beach, Virginia.

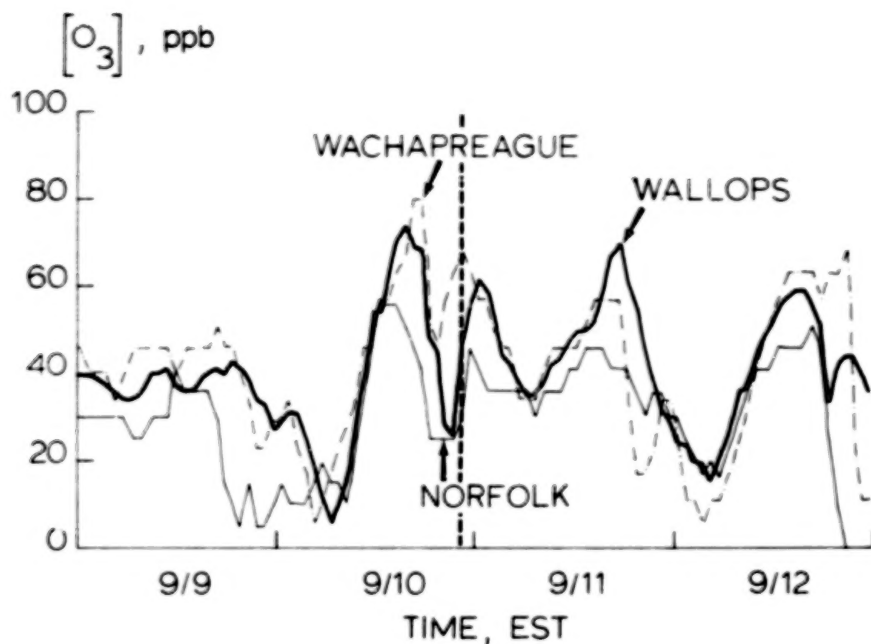


Figure 7. Surface ozone concentration variations at Wallops Flight Center, Wachapreague, Virginia, and the Norfolk International Airport during the period of the experiment. The time of the cold frontal passage at Wallops is indicated by the dashed vertical line.

DOBSON SPECTROPHOTOMETER DATA

During September 8-13, Dobson spectrophotometer data were taken, as usual, at three nominal times during the daylight hours - 1500, 1630 and 2000 GMT. Additionally, a series of measurements were taken each day near local noon with a spacing of 2-3 minutes. In Figure 8, these data are plotted versus time. The points shown with error bars are the average values of each series of measurements with the smaller error bars depicting plus and minus one standard deviation around the mean for each series. The exterior bounds on these data show the 5% nominal accuracy given by Thomas and Holland¹² as the ultimate capability of the Dobson spectrophotometer. The points without error bars are the single measurements made before and after local noon. They are, of course, subject to the 5% accuracy limitations as are the ensemble averages. No marked trends during the data collection period can be seen in these data.

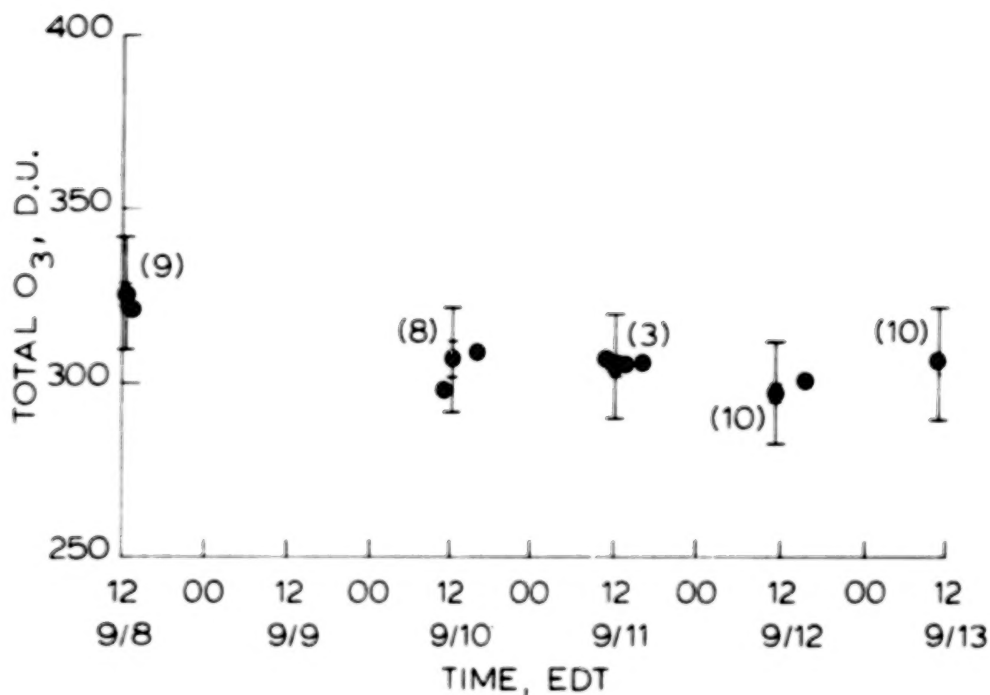


Figure 8. Wallops Dobson spectrophotometer measurements of total ozone overburden taken during the experiment. Data points with error bounds are ensemble averages with the number of individual values in each ensemble shown in parentheses. The interior error bars are the standard deviations from the average and the exterior bounds represent the $\pm 5\%$ errors typical of Dobson performance according to Thomas and Holland.¹⁵

ECC OZONESONDE DATA

Data Verification

Because no other method exists for obtaining high resolution ozone profiles in the altitude ranges covered by the WFC balloons, it is not possible to compare the vertical profiles obtained from the ozonesondes released at Norfolk and WFC during September 9-12, 1977, with other proven measurements. It is, however, possible to intercompare the profiles from each pair of simultaneous balloon releases to assess the combined effects of ECC ozonesonde consistency and horizontal atmospheric variability. These intercomparisons will be the subject of the following section. First, though, there are two other independent checks of the profile data quality that can be employed.

Surface ECC Ozonesonde and Dasibi Monitor Measurement Comparisons. Immediately prior to release, a balloon-borne ECC ozonesonde measures the ground-level concentration of ozone. At WFC, where a well-calibrated Dasibi Optical Ozone Monitor is continuously in operation, these surface readings can be compared with the Dasibi output. The results are shown in Figure 9. The ECC ozonesonde values have been converted from units of micro-millibars (μmb) to parts per billion (ppb) to correspond to the Dasibi measurements and

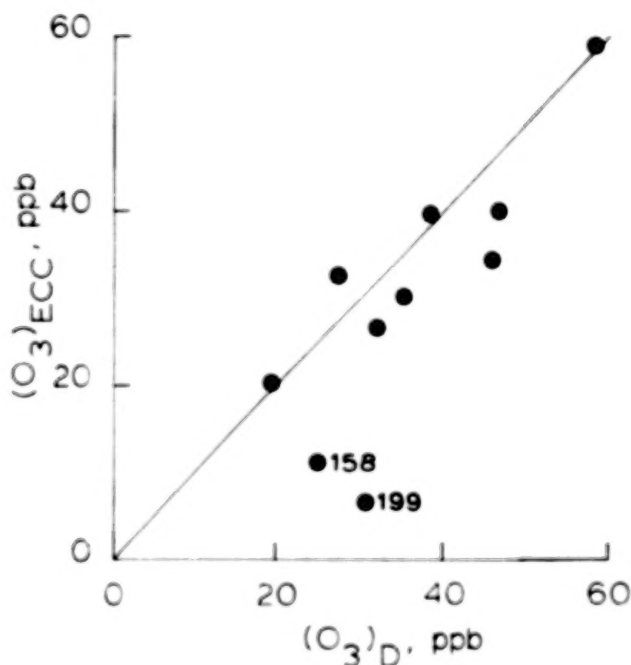


Figure 9. Intercomparison of the surface readings, $(\text{O}_3)_{\text{ECC}}$, from ECC ozonesondes released from Wallops Island with the coincidental Dasibi measurements, $(\text{O}_3)_D$.

the latter have been adjusted using equation 1 to achieve an absolute calibration. The ten points are from the WFC ozonesondes identified in Table I with the exception of 3A-081, which apparently suffered an instrumentation malfunction, and 3A-182, which first telemetered data at an altitude of 792 mb. It can be seen in the figure that eight of the ten points lie close to the 45 degree line signifying perfect agreement between the two measurement systems. The remaining points fall below the line indicating that the ozonesonde values were lower than those registered by the Dasibi. The measurement values along with the corresponding windspeed and direction data from the National Weather Service are tabulated in Table II. It can be seen that the wind data for sondes 3A-158 and 3A-199, the abnormal points in Figure 9, are in basic agreement. Hence, an explanation is not available for the discrepancies although interference from automobile traffic or other anthropogenic sources is always a concern.

TABLE II. Surface Comparison Data

WFC Sonde No.	Date	Time (EDT)	Island Data			Mainbase Data		
			(O ₃) _{ECC} (ppb)	U (kt)	θ	(O ₃) _D (ppb)	U (kt)	θ
3A-153	9/9	2200	32.8	2	110	27.4	4	160
3A-158	9/10	0200	11.2	9	260	25.0	6	250
3A-159	9/10	1100	26.5	16	290	32.0	10	310
3A-167	9/10	1600	59.0	11	290	58.4	6	--
3A-192	9/11	0200	40.8	14	340	46.8	10	--
3A-194	9/11	1100	30.0	13	320	35.1	13	--
3A-195	9/11	1600	34.2	13	300	46.0	10	--
3A-199	9/11	2200	6.4	5	320	30.5	4	--
3A-201	9/12	0200	20.4	8	10	19.6	7	--
3A-202	9/12	1100	39.6	6	340	38.3	6	360

ECC Ozonesonde and Dobson Spectrophotometer Total Ozone Measurement Comparisons. In addition to the comparison using the surface reading from an ozonesonde, the presence of the Dobson spectrophotometer at the site of the balloon releases at Wallops Flight Center facilitates a comparison of its total ozone measurement with the total overburden computed from the ozonesonde profile data. The latter is calculated as follows. In some layer between altitudes Z_1 and Z_2 , at which the air pressure is p_1 and p_2 , respectively, the ozone amount is given by

$$X_{12} = \frac{1}{\rho_{3\text{STP}}} \int_{Z_1}^{Z_2} \rho_3 dz \quad (2)$$

where X is the total ozone amount in atm-cm, ρ_3 is the density of ozone, and $\rho_{3\text{STP}}$ is the ozone density at standard temperature and pressure. Using the hydrostatic equation for the atmosphere

$$dp = -g\rho_a dz \quad (3)$$

equation (2) becomes

$$X_{12} = -\frac{1}{g\rho_{3\text{STP}}} \int_{p_1}^{p_2} \frac{\rho_3}{\rho_a} dp \quad (4)$$

where ρ_3/ρ_a is the ozone mixing ratio. Substituting for ρ_a , the density of dry air, from the equation of state yields

$$X_{12} = - \frac{1}{g \rho_{3\text{STP}}} \int_{p_1}^{p_2} \rho_3 R_a T \frac{dp}{p} \quad (5)$$

Also, it is useful to observe that the gas constant for ozone, R_3 , is given by

$$R_3 = \frac{R^*}{m_3} = R_a \frac{m_a}{m_3} = .6035 R_a \quad (6)$$

Substituting (6) in (5) results in

$$X_{12} = \frac{1.657}{g \rho_{3\text{STP}}} \int_{p_2}^{p_1} p_3 d \ln p \quad (7)$$

p_3 , the partial pressure of ozone, p_1 , and p_2 are all outputs of the ECC ozonesonde allowing for the calculation of the total ozone overburden in the vertical column above the balloon release point. Equation (7) was used for each of the twenty-one acceptable sondes identified in Table I. The resulting total ozone amounts expressed in Dobson units are tabulated below in Table III.

TABLE III. ECC Ozonesonde Total Ozone Amounts

Date	Approximate Release Time (GMT)	Norfolk Sonde		Wallops Sonde	
		Number	X_{ECC} (D.U.)	Number	X_{ECC} (D.U.)
9/9	2000	3A-169	317		
9/10	0200	3A-170	278	3A-153	295
9/10	0600	3A-171	290	3A-158	292
9/10	1500	3A-181	314	3A-159	275
9/11	0200	3A-185	295	3A-182	344
9/11	0600	3A-186	283	3A-192	293
9/11	1500	3A-187	305	3A-194	299
9/11	2000	3A-188	305	3A-195	285
9/12	0200	3A-189	319	3A-199	277
9/12	0600	3A-190	293	3A-201	314
9/12	1500	3A-191	295	3A-202	322

Above the burst altitude of the balloons, it was necessary to assume that the mixing ratio was constant, an assumption usually quite reasonable if the final report from the ozone-sonde was from an altitude well above a well-defined ozone maximum. By modifying equation (4) to represent a constant mixing ratio, it can be shown that the residual ozone amount above burst height can be calculated from the equation

$$X_{\text{res}} = 1.657 p_3 / g \rho_{3\text{STP}} \quad (8)$$

The total ozone amounts are also plotted in Figure 10 along with the Dobson measurements of Figure 8. Only the average Dobson reading taken at local noon on the days of the experiment are shown. Again, these are pictured with a 5% nominal error bound, and an 8% bound is shown on the total integrated amounts from the ozonesonde profiles reflecting the preliminary comparison work of Torres and Bandy.¹⁵ It can be seen that the balloon data is in reasonably good agreement with the Dobson measurements throughout the experiment. No systematic variation in the former is noted. For example, night-time releases do not

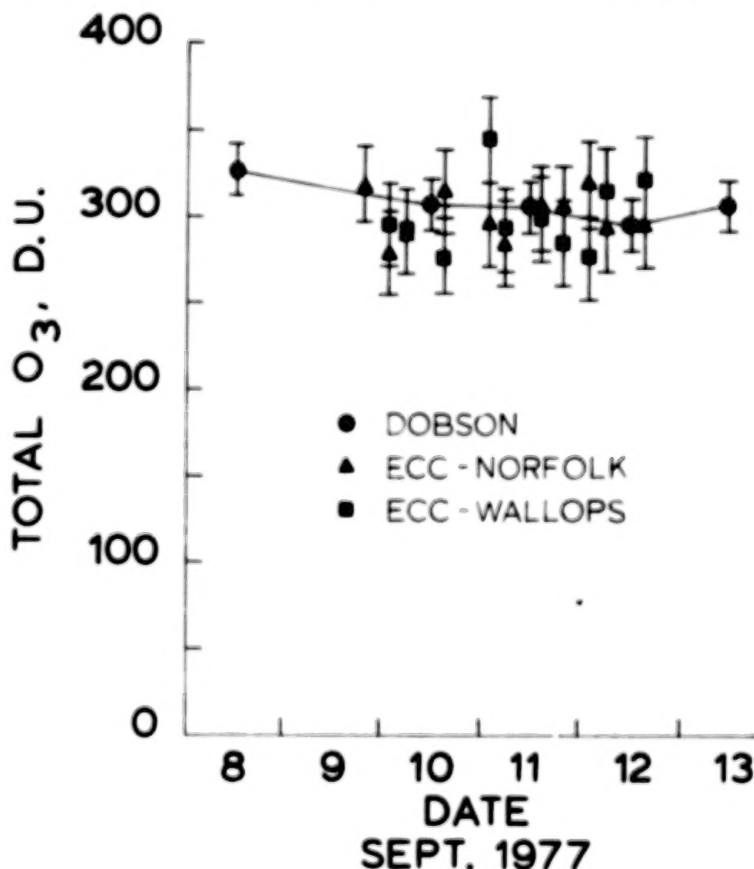


Figure 10. Intercomparison of the total ozone overburden computed by integration of the ECC ozonesonde profiles with the ozone amounts measured by the Wallops Dobson spectrophotometer.

appear to detect total ozone amounts different than the day-time balloons within the accuracy of the measurement technique. For the ten pairs of simultaneous balloon releases from Norfolk and Wallops, the computed values of ozone overburden differed by only 3 Dobson units on the average (i.e., $1 \text{ D.U.} = 10^{-3} \text{ atm cm}$) with the Wallops values slightly higher. The standard deviation of the differences was 28 D.U. Much of this scatter was undoubtedly the result of the imprecision and inaccuracy of the ECC ozonesonde.

Norfolk-Wallops ECC Ozonesonde Profile Comparisons

It has been shown that the surface ozonesonde readings are in good agreement with Dasibi measurements and that the total integrated ozone amounts agree with Dobson spectrophotometer reports. In Figures 11a-1, the individual profiles from both Norfolk and Wallops are displayed. When a pair of balloons were released successfully and simultaneously at the two stations, the profiles are both shown in the same figure for comparison. In general, the agreement between the member profiles of a pair is good. When differences do occur, they are in general small and they may exist throughout the profiles or may only be found in specific portions of the atmosphere. For example, in Figure 11d, the pair are nearly identical until the balloons reached the ozone maxima near 30 mb. Then the Norfolk sonde measured higher ozone partial pressure than did the Wallops instrument. Ozonesondes 3A-187 and 3A-194 were in consistently good agreement throughout their flights.

The greatest differences are found in Figure 11f where ozonesonde 3A-182 measured an abnormally high partial pressure of ozone at the ozone maximum, but was in good agreement with Norfolk ozonesonde 3A-185 elsewhere. No known instrument effects would cause the peak to be enhanced without the difference also occurring either above or below the ozone maximum. If it is a real increase in the ozone partial pressure, what physical mechanism is responsible? This pair of profiles will be discussed in some detail for several reasons. First, the large apparent enhancement of the ozone partial pressure at the ozone maximum caused the integrated ozone amount of ozonesonde 3A-182 to differ from its Norfolk counterpart by 16%, the largest such difference seen in Table III. In Figure 10, the 3A-182 point can also be seen to differ from the Dobson measurements by more than any other sonde result. Secondly, the pair of balloons in Figure 11f were released on September 10 at about 2200 EDT, one hour prior to the passage of the surface cold front at Wallops Island, Virginia.

Frontal Effects. By utilizing the isentropic cross sections presented earlier, the actual flight of the balloon can be charted through the existing structure of the atmosphere. Using standard radiosonde techniques, the tracking data from the ozonesonde receiver can be processed to yield measurements of the azimuth and elevation of the

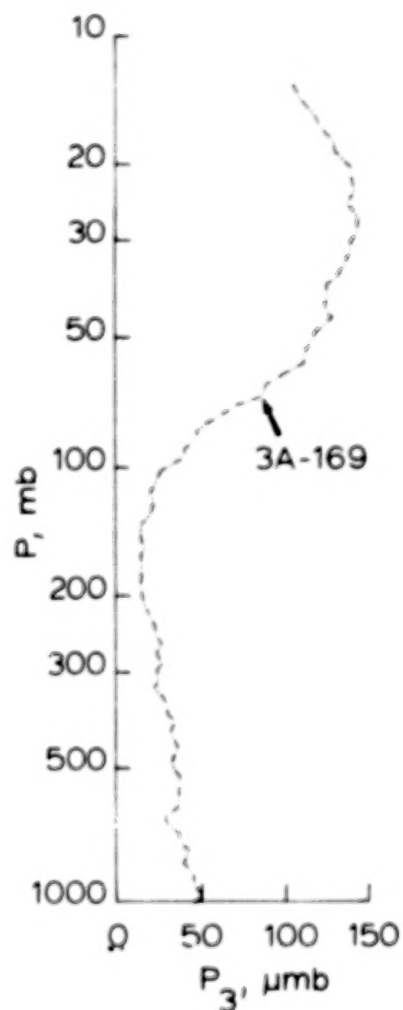


Figure 11(a)

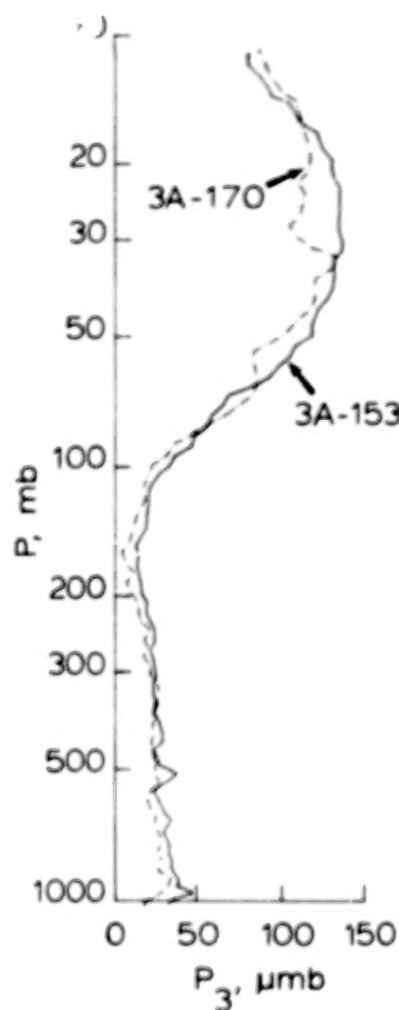


Figure 11(b)

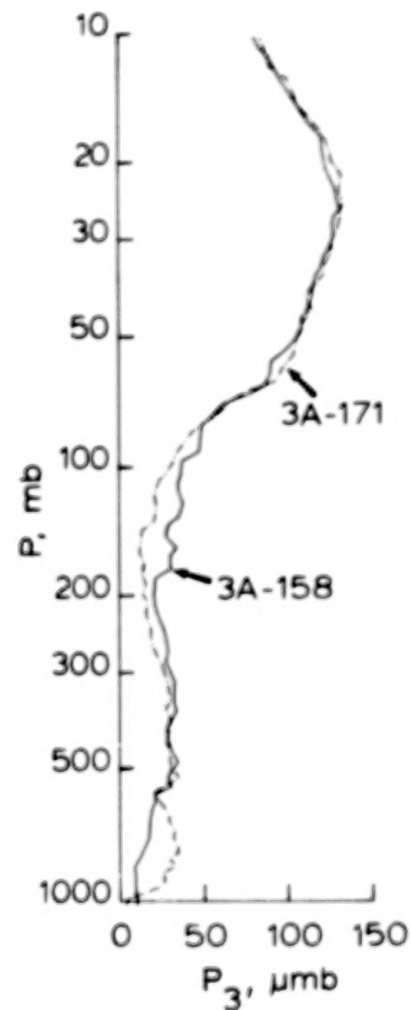


Figure 11(c)

Figure 11. ECC ozonesonde profiles. The ozonesondes released from Wallops Island produced the solid distributions and those launched at Norfolk International Airport produced the dashed profiles. The release times for the profiles in each figure are given in Table I.

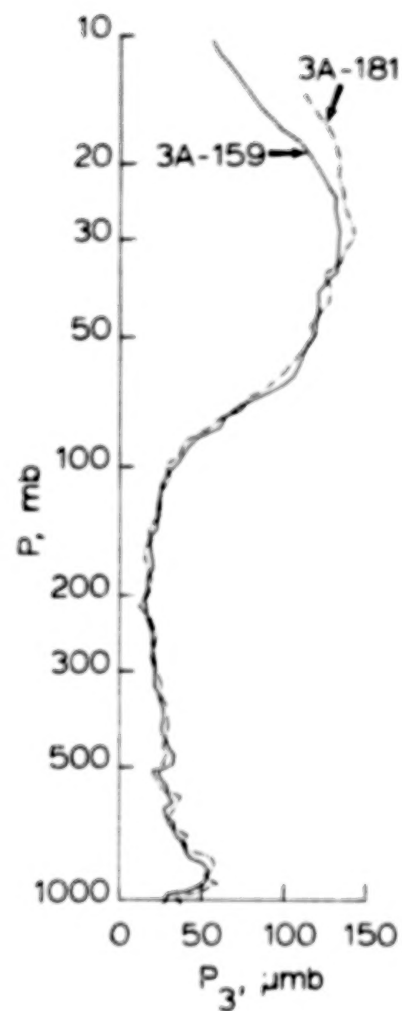


Figure 11(d)

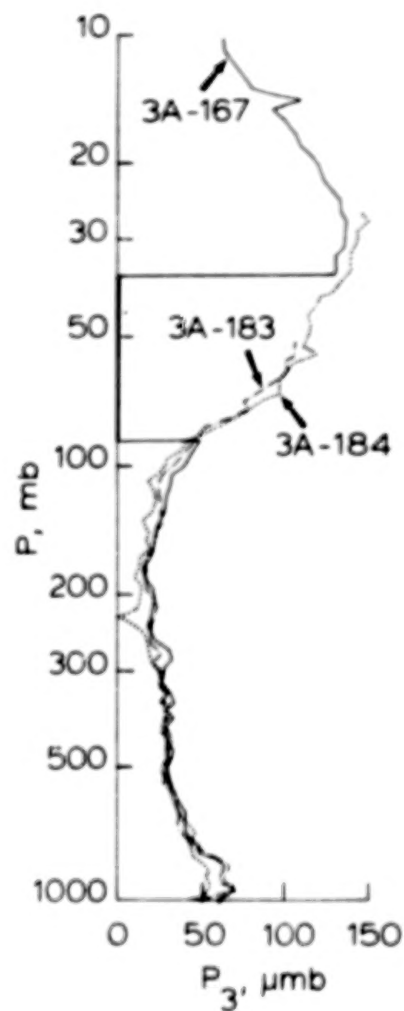


Figure 11(e)

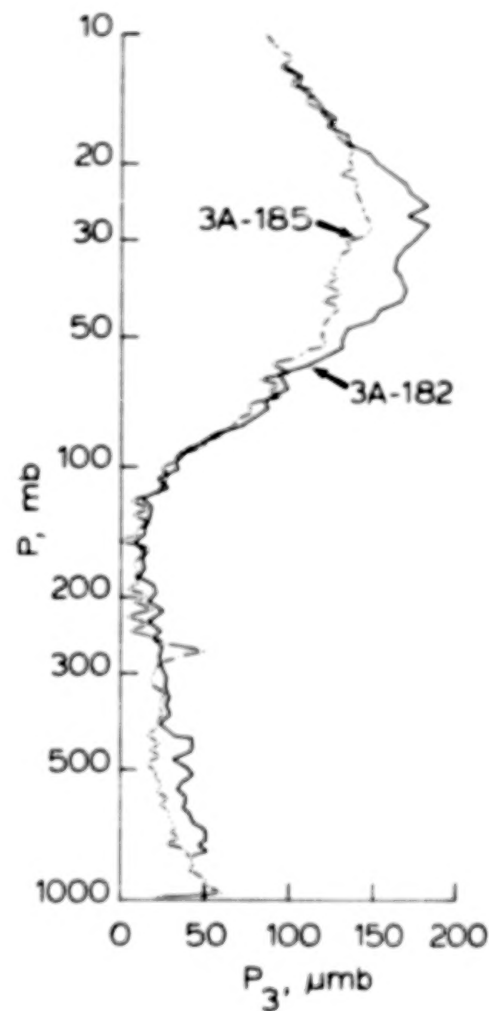


Figure 11(f)

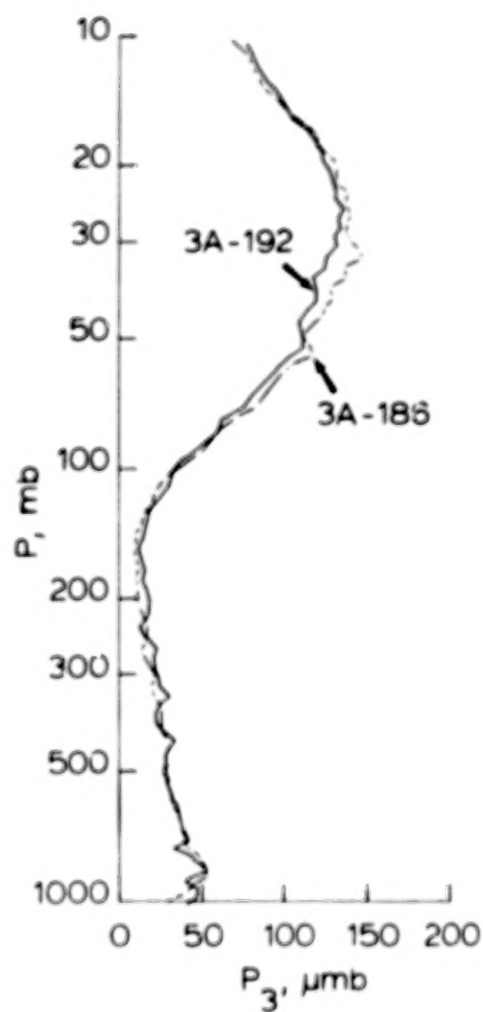


Figure 11(g)

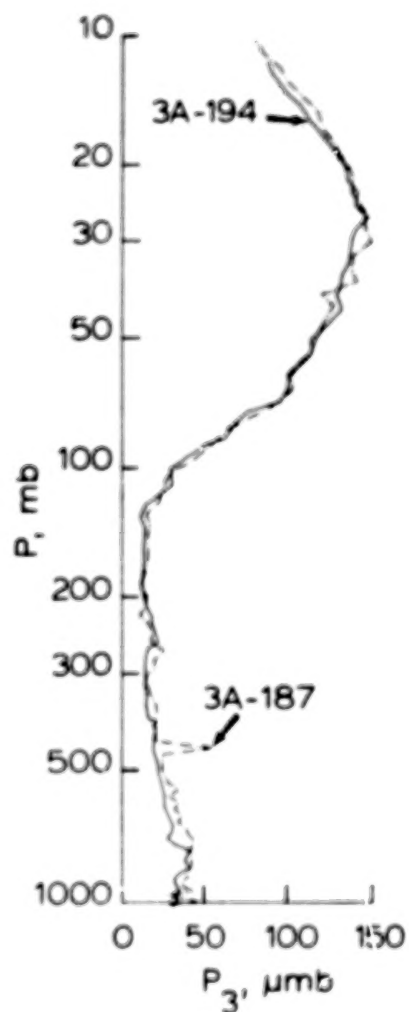


Figure 11(h)

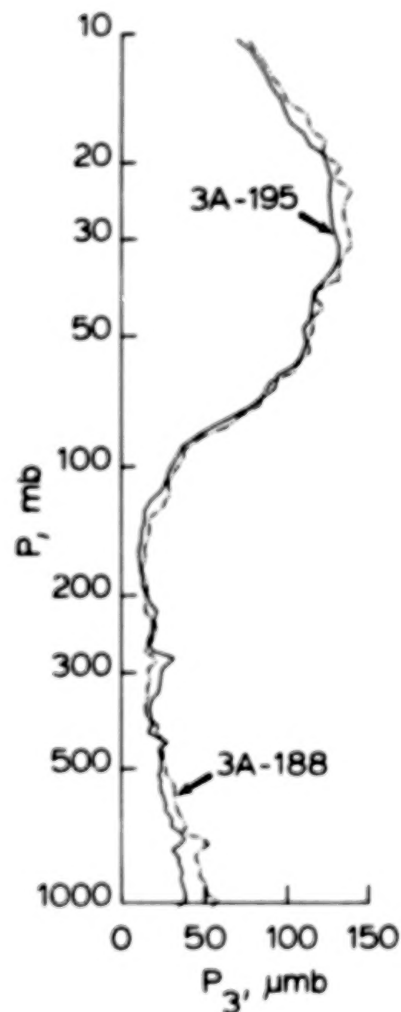


Figure 11(i)

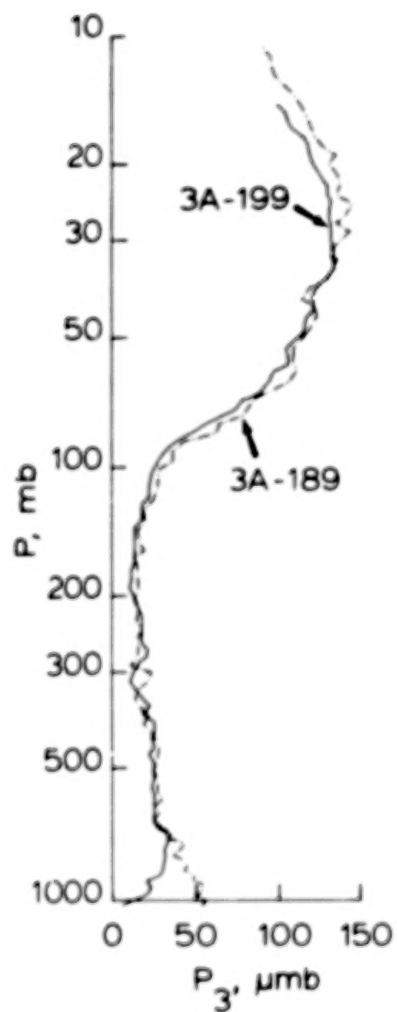


Figure 11(j)

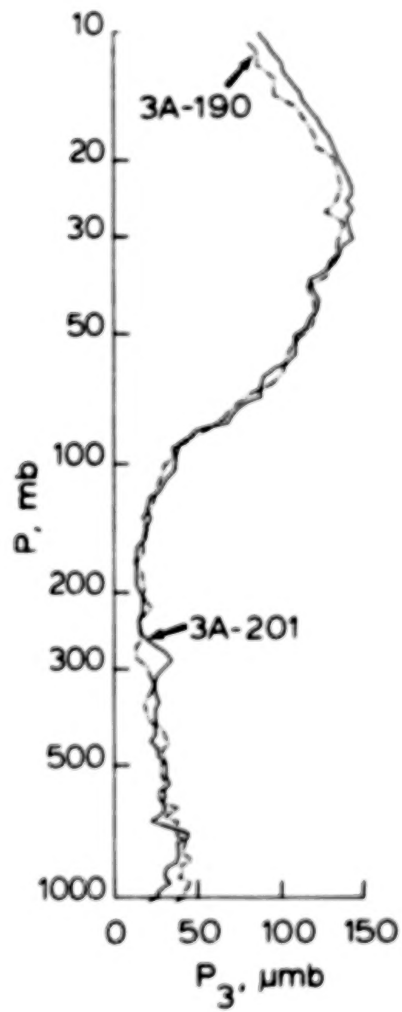


Figure 11(k)

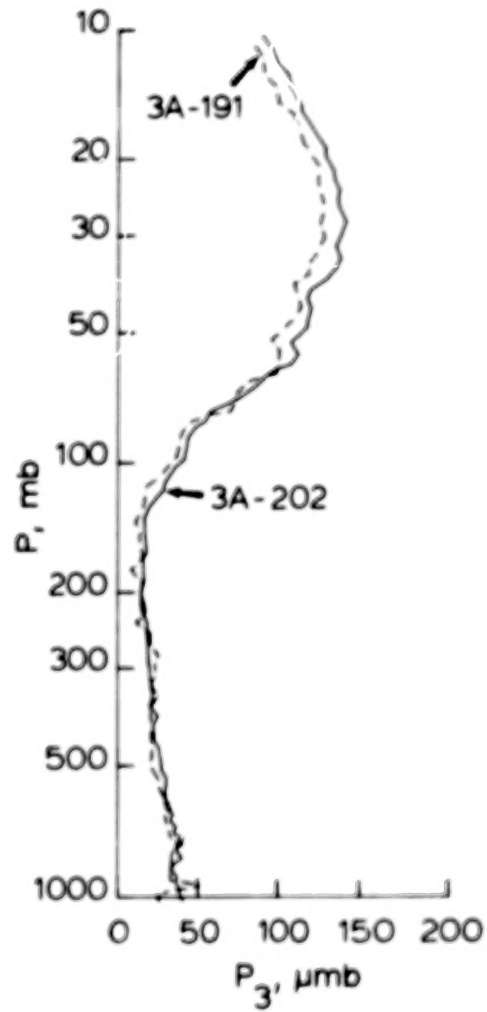


Figure 11(l)

balloon as a function of elapsed flight time. Knowledge of the ambient pressure in the vicinity of the ozonesonde results in a calculation of the balloon's altitude using the hypsometric formula. That value coupled with the measured elevation angle can be used to compute the range of the balloon from its release point and that result with the azimuth of the balloon pin-points the location of the balloon's nadir on the earth's surface. In Figure 12, the component of the vector from Wallops Island to the balloon's nadir spot in the direction perpendicular to the surface cold front is plotted on the right-hand portion of Figure 4, the isentropic cross section for 0000 GMT on September 11, 1977. Because this depiction of the atmosphere's structure is applicable approximately two hours earlier than the balloon's release, the profile has been translated one sixth of the distance between station 5 on the cross section, Wallops Island, and station 4, Dulles International Airport. As the balloon ascended, it was carried off of the coast in advance of the cold front. However, after about an hour of elapsed flight time, the balloon's motion was nearly vertical, and, thereafter, it was carried back towards its release point. No extrusions of stratospheric air can be found in Figure 12 and as noted earlier the upper air jet stream and the frontal system itself were weak and near complete dissipation. From Figure 10, it can be seen that no change in the computed total ozone overburden can

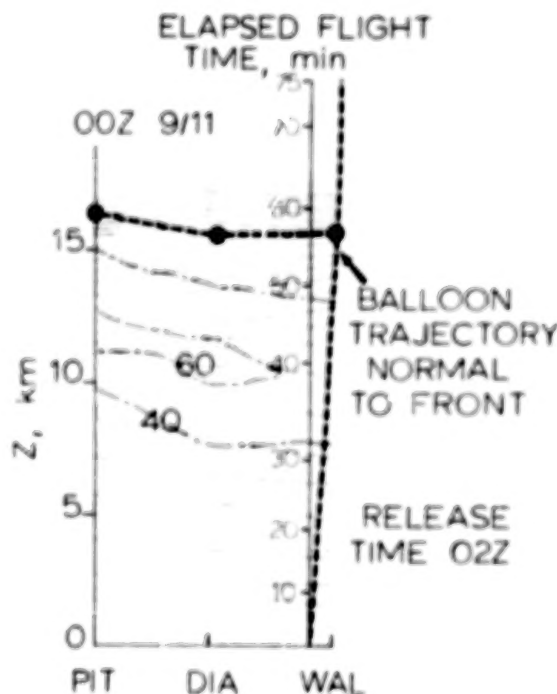


Figure 12. Superposition of the location of ECC ozonesonde 3A-182 normal to the cold front as a function of elapsed flight time on the isentropic cross section for 0000 GMT, September 11, 1977.

be associated with the frontal passage. It can only be speculated that the effects of a more intense frontal system may not be as negligible as were the results of this experiment. The only unusual condition seen in the ECC ozonesonde data that may be associated with the frontal passage is the enhanced ozone maximum for sonde 3A-182 and no connection between them is at present known. Plotted in Figure 13 are all of the meteorological measurements made by ozonesonde 3A-182 including the ozone partial pressure, the ambient air temperature, the lapse rate, the windspeed, and wind direction. Superimposed on the ozone data is the balloon location vector component in the direction perpendicular to the cold front that was described previously and shown in Figure 12. The prevailing westerly winds at altitudes below 70 mb are obviously responsible for the balloon's movement out to sea and the wind's reversal near the ozone maximum results in the translation of the balloon back towards Wallops Island. An analysis of these same ancillary measurements for each of the other ozonesondes released in this experiment has revealed no unusual meteorological activity that correlates with the enhanced maximum.

Stratospheric Wave Effects. The possible role of atmospheric waves on the dynamics of the lower stratosphere cannot be discounted. Recently, Vaughan²⁵ has discussed the applicability of a quasi-inertial oscillation model for explaining mesoscale wind phenomena observed in Jimsphere measurements. Variations of the wind data collected from the ECC ozonesondes flown at Wallops during this experiment match expected characteristics for this class of wave motion caused by a balance between inertial, Coriolis, and static stability effects. Sawyer²⁶ originally described these periodic wind variations with height as having vertical dimensions of the order of 1-2 km and horizontal dimensions of at least several hundred kilometers. Many characteristics of quasi-inertial oscillations are unknown, however. The motion of air parcels within the wave cannot be adequately measured in an Eulerian system as was used here because the advection associated with the oscillation is not seen. Without this knowledge, it is difficult to speculate on the effect of these waves on the mixing of ozone-rich air from the middle stratosphere with the ambient air in the lower stratosphere. The importance of atmospheric waves and the dynamics of the lower stratosphere on the ozone profile cannot be discounted and should receive attention in the future.

Photochemical Effects. Hesstvedt²⁷ used perturbation techniques to derive expressions for the time constant as a function of altitude of the restoration of photochemical equilibrium in the stratosphere. Using these results, it is possible to simulate the resultant ozone profile as a function of time after a vertical displacement of the original photochemical equilibrium concentration profile. The results of a simple numerical simulation are shown in Figure 14. The atmosphere was divided into ten 5 km thick layers from the surface to 50 km. The equilibrium profile is taken from Hesstvedt²⁷ and the seasonally averaged mid-latitude ozone profile is from the 1976 U.S. Standard Atmosphere.²⁸ Three other curves are also in the illustration. If 1/2 of the ozone concentration in each

25

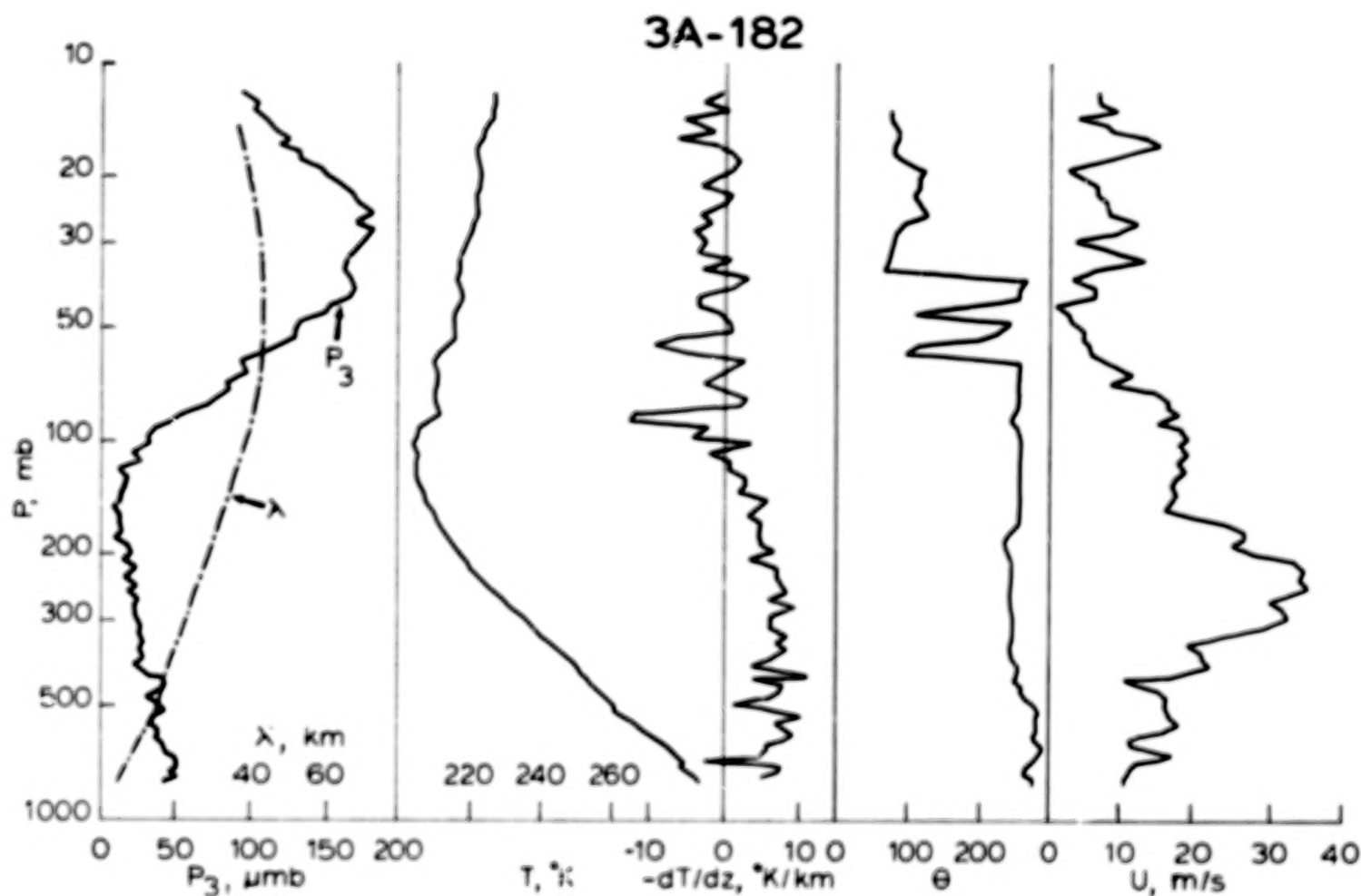


Figure 13. Vertical variations of ozone partial pressure, p_3 , temperature, T , lapse rate, $-dT/dz$, wind direction, θ , and windspeed, U , for ozonesonde 3A-182. Superimposed on the vertical distribution of ozone is the balloon position normal to the cold front, λ , shown in Figure 12.

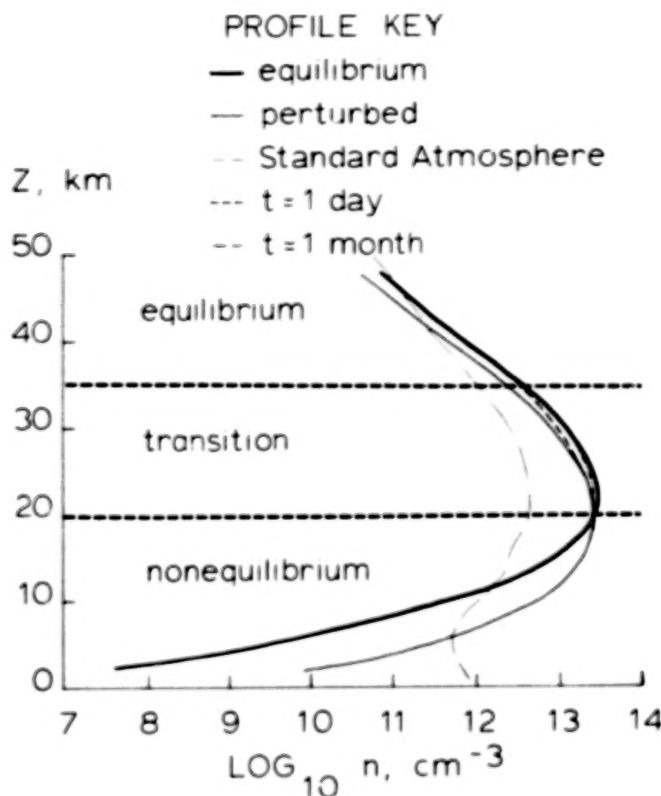


Figure 14. Results of a simulation showing the effect of photochemistry on a perturbed vertical distribution of ozone. The photochemical equilibrium profile and the restoration time constants are from Hesstvedt.²⁷

layer is instantaneously lost to the layer immediately below it, the entire profile is displaced downwards. Utilizing Hesstvedt's results, however, the process of restoring photochemical equilibrium can be shown to begin immediately with the recovery occurring most rapidly in the upper stratosphere. At 50 km, one-half of the recovery is complete after about 1-1/2 hours, while at 30 km nearly 100 hours are required. Hence, in Figure 14, it is seen that after 1 day of displacement, restoration of equilibrium is complete down to the 35-40 km layer. Below 20 km, the perturbation of the original profile is still unaffected by photochemical activity. After 1 month, the equilibrium is restored down into the 25-30 km layer but little if any change has been made to the non-equilibrium profile below 20 km. Based on this crude model, it has been shown that full adjustment is made above 35 km, no adjustment is made below 20 km, and all transitional restoration effects occur in between, in the region of the ozone maximum.

Because the sampling interval for data collection in this experiment was approximately 6 hours, the mechanism responsible for the ozone maximum enhancement of sonde 3A-182 could not have been photochemical in nature. Any perturbation of the ozone profile at

an altitude of 25 km would persist for approximately one month before photochemical processes could overcome it and restore the profile to equilibrium. Therefore, the advection of ozone or ozone precursors into the path of 3A-182 appears to be the only physically reasonable mechanism for explaining its high peak reading. Because any dynamics responsible for its enhancement must also have caused its return to normal levels 4 hours later when ozonesonde 3A-192 was released, this explanation too seems far-fetched.

CONCLUSIONS

Twenty-five Electrochemical Concentration Cell ozonesondes were released in pairs from Wallops Flight Center and Norfolk International Airport to evaluate their performance capabilities and to adjudge the spatial and temporal scales of ozone variability in the real atmosphere. In support, surface ozone concentration measurements from Dasibi Corporation Optical Ozone Monitors and total ozone overburden readings from a Dobson spectrophotometer were available at Wallops Flight Center. These latter ancillary measurements were used to verify acceptable performance by the ozonesondes. Eight of ten Wallops Flight Center ozonesondes had surface readings in excellent agreement with Dasibi measurements made at the same time about 5 miles distant. The low reading of the remaining two sondes is unexplained. When the total ozone overburden is computed by integrating under the 21 ozonesonde profiles and assuming a constant ozone mixing ratio above the balloon burst height, the agreement between the simultaneously released Norfolk and Wallops sondes is good with a mean difference of 2.8 D.U. and a standard deviation of the differences of about 28 D.U., or about 9%. When compared with a linearly interpolated Dobson measurement throughout the data collection period, the Wallops overburdens differ by 5.4 D.U. with a standard deviation of 23.4 D.U. and the Norfolk values differ by 6.4 D.U. with a standard deviation of 15.1 D.U. The conclusion from these intercomparisons is that the balloon-borne ECC ozonesondes are capable of measuring the vertical profile of ozone to within 10% of the actual value.

Part of the disagreement between the overburdens measured by the ozonesondes and the interpolated Dobson readings may be caused by real physical effects. Initial efforts towards identifying these features in the data have proved inconclusive, however. Neither the passage of the weak cold front through the Wallops region or the lack of insolation at night appears to cause a noticeable change in the total ozone measurements. That is, day-night variations and weak air mass changes appear to affect the total ozone overburden by amounts less than the 10% sensitivity limit of the ozonesonde measurement system.

This is not meant to imply, however, that physical mechanisms are not important. Day-night variations and air mass changes undoubtedly do play important albeit small roles in the natural variability of ozone in the atmosphere. The most puzzling feature of this experiment's data set is the enhanced ozone maximum during the flight of ozonesonde 3A-182. Although an instrumentation effect cannot be ruled out, no known hardware performance can account for this feature. Similarly, photochemical activity cannot be responsible because of the speed with which the anomaly disappears. The preliminary conclusion drawn from this experiment is that either the dynamics of the lower stratosphere or sporadic instrument effects may be responsible for significant variations in the vertical profile of ozone by ECC ozonesondes. Further study of the sonde's performance under conditions of low temperature and pressure is needed before the anomalous enhancement can be explained.

ACKNOWLEDGMENTS

The direction of the data collection by Harry Bloxom is gratefully acknowledged by the author. Numerous other significant contributions were made by colleagues at Wallops Flight Center.

REFERENCES

1. Molina, M. J. and Rowland, F. S., "Stratospheric Sink for Chlorofluoromethanes: Chlorine Atom-Catalysed Destruction of Ozone," Nature, 249, 810-812, 1974.
2. Smith, K. C. (Chairman, Ad Hoc Committee), Biological Impacts of Increased Intensities of Solar Ultraviolet Radiation. A Report to the Environmental Studies Board, National Academy of Sciences, Washington, DC, 1973.
3. Crutzen, P. J., "SST's, A Threat to the Earth's Ozone Shield," Ambio, 1, 41-51, 1972.
4. Crutzen, P. J., "The Influence of Nitrogen Oxides on the Atmospheric Ozone Content," Quart. J. Roy. Meteor. Soc., 96, 320-325, 1970.
5. Johnston, H. S., "Reduction of Stratospheric Ozone by Nitrogen Oxide Catalysts from SST Exhaust," Science, 173, 517-522, 1971.
6. Council on Environmental Quality/Federal Council for Science and Technology, Fluorocarbons and the Environment, Report of the Federal Task Force on Inadvertant Modification of the Stratosphere, U.S. Government Printing Office, Washington, DC, 1975.
7. Grobecher, A. J., Coroniti, S. C. and Cannon, R. H., CIAP Report of Findings, the Effects of Stratospheric Pollution by Aircraft, Department of Transportation DOT-TST-75-50 (Available through National Technical Information Service, Springfield, VA 22151), 1974.
8. Interdepartmental Committee for Atmospheric Sciences, A United States Climate Program Plan, ICAS 206-FY1977, Washington, DC, July 1977 (Available through National Climate Program Coordinating Office, Department of Commerce-NOAA-WSC-5, 6010 Executive Blvd., Rockville, MD 20852).
9. WMO-ICSU Joint Organizing Committee, The Physical Basis of Climate and Climate Modelling, GARP Publications Series No. 16, World Meteorological Organization, Geneva, 1975.
10. Interdepartmental Committee for Atmospheric Sciences, The Possible Impact of Fluorocarbons and Halocarbons on Ozone May 1975, ICAS 18a-FY 75, U.S. Government Printing Office, Washington, DC, 1975.
11. Dobson, G. M. B., Ozone Spectrophotometer Operations Manual, Vol. 5, Part 1: Annals of the International Geophysical Year, Pergamon Press, Oxford, 1961.
12. Thomas, R. W. L. and Holland, A. C., "Ozone Estimates Derived from Dobson Direct Sun Measurements: Effect of Atmospheric Temperature Variations and Scattering," Applied Optics, Vol. 16, 613-618, 1977.
13. Ozone Monitor Operating and Instruction Manual, Dasibi Environmental Corporation, Glendale, California.
14. Hodgeson, J. A., A Survey of Calibration Techniques for Atmospheric Ozone Monitors, NBSIR 76-1191, 1976.

15. Torres, A. L. and Bandy, A. R., Performance Evaluation of Electrochemical Concentration Cell Ozonesondes, Final Report, NASA/WFC Grant No. NSG-6007, 1977.
16. Komhyr, W. D., "A Carbon-Iodine Sensor for Atmospheric Soundings," Proc. Ozone Symposium, WMO, Albuquerque, NM, 1964.
17. Komhyr, W. D. and Harris, T. B., "Development of an ECC Ozonesonde," NOAA Technical Report ERL-APCL 18, Boulder, Colorado, 1971.
18. Dobson, G. M. B., Harrison, D. N., and Lawrence, J., "Measurements of the Amount of Ozone in the Earth's Atmosphere and Its Relation to Other Geophysical Conditions," Pt. I - Proc. R. Soc., Ser. A, Vol. 110, No. 756: 660-692, 1926; Pt. II - Ibid, Vol. 114, No. 768: 521-541, 1927; Pt. III - Ibid, Vol. 122, No. 790: 456-486, 1929; Pt. IV - Ibid, Vol. 129, No. 811: 411-433, 1929.
19. Cahir, J. J., Norman, J. M., Lottes, W. D., and Toth, J. A., "New Tools for Forecasters: Real-Time Cross Sections Produced in the Field," Bull. Amer. Meteor. Soc., Vol. 57, No. 12, 1426-1433, 1976.
20. Staley, D. O., "Evaluation of Potential-Vorticity Changes Near the Tropopause and the Related Vertical Motions, Vertical Advection of Vorticity, and Transfer of Radioactive Debris from Stratosphere to Troposphere," J. Meteor., Vol. 17, 591-620, 1960.
21. Rees, R. J. and Danielsen, E. F., "Fronts in the Vicinity of the Tropopause," Arch. Meteorol. Geophys. Bioklimatol., SAB11, 1-17, 1959.
22. Danielsen, E. F., "Stratospheric-Tropospheric Exchange Based on Radioactivity Ozone, and Potential Vorticity," J. Atmos. Sci., 25, 502-518, 1968.
23. Danielsen, E. F. and Mohnen, Volker A., "Project Dust Storm Report: Ozone Transport, In Situ Measurements, and Meteorological Analysis of Tropopause Folding," J. Geophys. Res., Vol. 82, No. 37, 5867-5877.
24. Frank, A. E., and Barber, D. A., "Fronts and Frontogenesis as Revealed by High Time Resolution Data," NASA Reference Publication 1005, August 1977.
25. Vaughan, W. W., "An Investigation of the Temporal Character of Mesoscale Perturbations in the Troposphere and Stratosphere," NASA TN D-8445, Wash., D.C., March 1977, 87 pp.
26. Sawyer, J. S., "Quasi-Periodic Wind Variations with Height in the Lower Stratosphere," Quart. J. Roy. Meteor. Soc., Vol. 87, pp. 24-33, 1961.
27. Hesstvedt, E., "On the Determination of Characteristic Times in a Pure Oxygen Atmosphere," Tellus, XV, 1, 1963, pp. 82-95.
28. U.S. Standard Atmosphere, 1976, NOAA, NASA, USAF, Wash., D.C., October 1976, 227 pp.

1. Report No. TP-1239		2. Government Accession No.		3. Recipient's Catalog No.	
4. Title and Subtitle AN EVALUATION OF IN SITU OZONE SENSOR PERFORMANCE DURING A COLD FRONTAL PASSAGE				5. Report Date July 1978	
				6. Performing Organization Code	
7. Author(s) C. L. Parsons				8. Performing Organization Report No.	
				10. Work Unit No.	
9. Performing Organization Name and Address National Aeronautics and Space Administration Wallops Flight Center Wallops Island, VA 23337				11. Contract or Grant No.	
				13. Type of Report and Period Covered	
12. Sponsoring Agency Name and Address National Aeronautics and Space Administration Wallops Flight Center Wallops Island, VA 23337				14. Sponsoring Agency Code	
15. Supplementary Notes					
16. Abstract <p>The capabilities of the Electrochemical Concentration Cell ozonesonde for measuring the vertical profile of atmospheric ozone were studied during a three-day experiment at Wallops Island, Virginia, and Norfolk, Virginia. Using ancillary measurements by Dasibi Corporation Optical Ozone Monitors at the surface and the Wallops Island Dobson spectrophotometer, it was concluded that the ozonesonde measures the total ozone overburden to within 10% of the real value.</p> <p>By releasing the balloon-borne instruments at a rate of four per day at each of the two sites, an indication was obtained of the temporal and spatial scales of atmospheric ozone variability. No significant effects of a weak cold front passage or of the loss of insolation at night were seen. An isolated incident of anomalously high ozone concentration at the peak of the profile has been attributed to sporadic instrument performance effects. The data base currently available is not adequate for determining an exact cause of the anomaly.</p>					
17. Key Words (Suggested by Author(s)) Ozone Atmospheric Composition Balloon-Borne Instruments Radiosondes Climatology			18. Distribution Statement Unclassified - Unlimited STAR Category 47		
19. Security Classif. (of this report) Unclassified		20. Security Classif. (of this page) Unclassified		21. No. of Pages 31	
				22. Price* \$4.50	

90

50